International Immunopharmacology 77 (2019) 105929

Contents lists available at ScienceDirect

International Immunopharmacology

journal homepage: www.elsevier.com/locate/intimp

Ethyl pyruvate enhances spontaneous remyelination by targeting microglia phagocytosis

Yan He[a], Jun An[a], Jun-Jun Yin[a], Ruo-Xuan Sui[a], Qiang Miao[a], Zhi-Bin Ding[a], Qing-Xian Han[a], Qing Wang[a], Cun-Gen Ma[a,b,*], Bao-Guo Xiao[c,*]

[a] The Key Research Laboratory of Benefiting Qi for Acting Blood Circulation Method to Treat Multiple Sclerosis of State Administration of Traditional Chinese Medicine, Shanxi University of Chinese Medicine, Taiyuan 030024, China
[b] Institute of Brain Science, Shanxi Datong University, Datong 037009, China
[c] Institute of Neurology, Huashan Hospital, Institutes of Brain Science and State Key Laboratory of Medical Neurobiology, Fudan University, Shanghai 200025, China

ARTICLE INFO

Keywords:
Ethyl pyruvate
Cuprizone-induced demyelination
Microglia
Phagocytosis
Remyelination

ABSTRACT

Ethyl pyruvate (EP), a simple derivative of the endogenous energy substrate pyruvate, provides strong anti-inflammatory and anti-oxidative properties. but its role in remyelination has not been explored. In this study, EP efficiently improved the behavioural performance and histological demyelination in cuprizone (CPZ)-induced mouse model. In terms of action, EP treatment enhanced microglia migration, increased the phagocytosis of myelin debris by BV2 microglia and primary microglia, induced cell proliferation and subsequent cell death. At the same time, EP induced microglia to exhibit M2 phenotype, representing decreased iNOS/TNF-α and increased Arg-1/IL-10. In addition, EP decreased microglia enrichment in myelin sheath, and declined TLR4/p-NF-kb/p65 and IL-1β and IL-6, inhibiting microglia-mediated neuroinflammation. As a result, EP treatment promoted the generation of oligodendrocyte progenitor cells (OPCs) and the differentiation from maturation to mature oligodendrocytes, which may be related to the up-regulation of Sox2. Given these data, we provided the proof-of-experiment that EP should be beneficial in multiple sclerosis or demyelinating lesions. However, further studies on the possibility to use EP as therapeutic application are warranted.

1. Introduction

The neuroinflammation and demyelination are two main pathological phenomena of multiple sclerosis (MS). Although the pathogenetic process of leading to oligodendrocyte loss and subsequent demyelination has not been fully elucidated, but several hypotheses are proposed, including inflammatory response, oxidative stress, mitochondrial dysfunction, or protein misfolding [1,2]. Currently, although there is no cure for MS patients, several disease-modifying therapies (DMTs) have become available in the relapsing form of MS [3]. A series of studies have demonstrated that relapses are driven by focal inflammatory demyelination, leading to oligodendrocyte loss and axonal injury [4]. Remyelination restores axonal conduction and contributes to clinical recovery [5]. Therefore, novel therapeutic strategies targeting remyelination and neuroprotection are two unmet needs in the treatment of MS [6,7].

Ethyl pyruvate (EP), a simple derivative of the endogenous energy substrate pyruvate, provides strong anti-inflammatory and anti-oxidative properties [8]. In contrast to pyruvate, EP yielded a higher potency, most probably due to their more lipophilic properties and significant stability in vivo [8,9]. Despite the existence of chemical structural similarity, it is remarkable that differential pharmacological effects have been observed when EP and pyruvate have been compared head-to-head in models of inflammation and/or redox stress. Besides the anti-inflammatory effect, EP has been reported to be neuroprotective in several models of brain injury. Treatment with EP can improve survival and/or ameliorate organ dysfunction in a wide variety of experimental models of critical illnesses, including stroke [10], spinal cord injury [11] and Parkinson's disease [12]. In addition, EP was able to provide potent protection on white matter injury by blocking the inflammatory responses and modulating the apoptosis of oligodendrocytes [13]. So far, we have not found whether EP can protect or regenerate myelin sheath in demyelinating state.

Cuprizone (CPZ)-induced demyelination, unlike experimental autoimmune encephalomyelitis (EAE), is independent of autoimmune attack, and is also often used to mimic the pathology of human MS

* Corresponding authors at: The Key Research Laboratory of Benefiting Qi for Acting Blood Circulation Method to Treat Multiple Sclerosis of State Administration of Traditional Chinese Medicine, Shanxi University of Chinese Medicine, Taiyuan 030024, China (C.-G. Ma).
E-mail addresses: macungen2001@163.com (C.-G. Ma), bgxiao@shmu.edu.cn (B.-G. Xiao).

https://doi.org/10.1016/j.intimp.2019.105929
Received 22 May 2019; Received in revised form 3 September 2019; Accepted 21 September 2019
Available online 30 October 2019
1567-5769/

[14,15]. There are several similarities between CPZ-induced pathology and histopathological alterations as described in post-mortem MS material. For example, the density of mitochondria within demyelinated axons is increased in active MS lesions [16] and cuprizone-induced white matter lesions [17]. In addition, pre-apoptotic oligodendrocytes expressed active caspase-3 during the process of pathological lesions in MS [18] and CPZ-induced demyelination [19]. There is also a lack of therapeutic drugs in myelin protection or remyelination. Therefore, CPZ-induced demyelination provides a good experimental model to study demyelination and remyelination, and is a suitable pharmacological model for developing novel promising drugs of remyelination and/or neuroprotection.

Based on the multiple effects of EP in anti-inflammation and neuroprotection, an attempt to induce myelin protection and regeneration is reasonable and appropriate. In this study, we observed the therapeutic potential of EP in CPZ-induced demyelinating model and explored the possible cellular and molecular mechanisms of action.

2. Materials and methods

2.1. Animals

Male C57BL/6 mice (8–10 weeks) were purchased from Vital River Laboratory Animal Technology Co. Ltd. (Beijing, China). This study was approved by the Laboratory and Ethics Committee of Shanxi University of Traditional Chinese medicine, Taiyuan, China. All animal protocol was performed according to the guidelines of the International Council for Laboratory Animal Science. All mice were maintained and housed under pathogen-free conditions in a reversed 12:12 h light/dark cycle for one week prior to experimental manipulation.

3. CPZ-induced demyelinating model

Mice were fed with 0.2% (w/w) CPZ (Sigma-Aldrich, USA) in chow diet ad libitum for 6 weeks. After 4 weeks of CPZ feeding, mice were randomly divided into four groups (n = 8/group) as follows: (1) normal group fed a normal diet (Normal); (2) normal group injected with EP (Normal + EP); (3) CPZ group fed CPZ and injected with normal saline (CPZ) and (4) EP-treated group, which were intraperitoneally (i.p.) injected with EP (10 mg/kg), starting from fourth weeks until sixth weeks for consecutive 14 days (CPZ + EP).

4. Behavioral tests

Elevated plus-maze (EPM), forced swimming test (FST) and T-maze test were performed before the end of the experiment. EPM was used to measure anxiety levels of mice as they avoid the open arms of the plus-maze [20]. Briefly, the mice were placed individually in the center of the plus maze facing an open arm. The number of entering closed arms was recorded during 10-min testing period.

FST was carried out by previous report [21]. The mice were placed individually to swim in a plastic cylinder (height: 30 cm, diameter: 10 cm) filled with 20 cm of 25 ± 1 °C water. The total duration of the stress exposure and behavior were recorded during 1 min by digital video, and the mean swimming distance was analyzed by SNART V3.0 software (RWD Life Science Co. USA).

T-maze test for learning and memory was performed as described previously, with minor modifications [22]. The T-maze consisted of two arms and one stem. There was a start box on the bottom of the stem of the maze. Two target compartments were located at the end of both arms of the maze. Mice were tested 10 times per day for 3 days. Mice were positioned at the end of one stem and given the possibility to move for 10 min. Successive entry in each arm was considered as an alternation in behavior. Data acquisition and analysis were performed automatically using ImageTM software

5. Tissue preparation

Half of the mice in each group were anaesthetized with 10% chloralhydrate and perfused intracardially with saline, followed by 4% paraformaldehyde. Brains were removed and cryo-protected in 15%, 25%, and 30% sucrose solutions. Brain coronal sections (10 μm) were cut using a cryostat microtome (Leica CM1850, USA) for immunofluorescence staining. Another half of the mice were only anaesthetized with 10% chloralhydrate and perfused intracardially with saline. Brains were quickly removed and stored at − 80 °C for ELISA and western blot.

6. Myelin staining

Histological myelin staining was performed by Black Gold II and myelin basic protein (MBP) staining. For Black Gold II staining, brain sections were stained with Black Gold II (AG105, Millipore Corp, Billerica, MA) according to the manufacturer's instructions. Briefly, pre-warmed Black Gold II solution was added onto sections and incubated for 15 min at 60 °C. After washing with Milli-Q water, pre-warmed 1% sodium thiosulfate was added to the slides and incubated for 3 min, followed by the incubation with cresyl violet stain for 3 min. For MBP immunohistochemistry staining, brain sections were blocked with 1% BSA/PBS at RT for 30 min, stained with anti-MBP (Abcam, USA) for 18 h at 4 °C, and then incubated with corresponding secondary antibodies for 2 h at RT. Results were visualized under fluorescent microscopy in a blinded fashion. The mean density of Black Gold II and MBP staining in the corpus callosum was measured by Image-Pro Plus 6.0 software.

7. Immunohistochemistry

Brains sections were blocked with 1% BSA/PBS at RT for 1 h, and incubated with anti-MBP (Abcam, USA), anti-Iba-1 (BD Bioscience), anti-TLR4 (Bioworld Tech. Inc, USA), anti-p-NF-kB/p65 (Cell Signaling Technology, USA), anti-iNOS (Abcam, USA), anti-Arg1 (Gene Tex, USA), anti-O2 (R&D System, USA), ant anti-NG2 (Millipore, Germany) and anti-Sox2 (Abcam, USA) at 4 °C for overnight, followed by corresponding secondary antibodies at RT for 1 h. Additional sections were treated similarly, but the primary antibodies were omitted for negative control. Results were observed under fluorescence microscopy in a blinded fashion. Analysis and quantification were performed on three sections per mouse by Image-Pro Plus 6.0 software.

7.1. Western blot analysis

The brain extract (30 μg) was separated by sodium dodecyl sulfate-polyacrylamide gel electrophoresis (SDS-PAGE) and transferred electrophoretically to nitrocellulose membrane (Millipore). After blocking with 5% skimmed milk for 1 h at RT, the membranes were incubated with anti-MBP (Abcam, USA), anti-Iba1 (Abcam, USA), anti-NG2 (Abcam, USA) and anti-β-actin (Cell Signaling Technology, USA) at 4 °C for overnight, followed by HRP-conjugated secondary antibodies (Abcam, USA) at RT for 1 h. Immunoblots were developed with an enhanced chemiluminescence system (GE Healthcare Life Sciences) and measured using Quantity Software (Bio-Rad, Hercules, CA, USA). β-actin was used as an internal reference.

8. Cytokine ELISA assay

The concentrations of IL-1β, IL-6, IL-10 and TNF-α (R&D System, USA) were measured by sandwich ELISA kits following the manufacturer's instructions. Determinations were performed in duplicate in 3 independent experiments. The results were expressed as pg/ml.

9. BV2 microglia culture

The BV2 mouse microglia cell line (from ShenKe Biological Technology Co., Ltd., Shanghai, China) was cultured in Dulbecco's modified Eagle medium (DMEM, Gibco, Gaithersburg, MD) with 10% fetal bovine serum, 100U/ml penicillin, and 100 μg/ml streptomycin (complete medium) at 37 °C and a humidified atmosphere augmented with 5% CO_2. Cells were plated at a density of 1×10^5 /ml for all experiments. BV2 cells were counted by flow cytometry (Life technologies Attune Nxt acoustic focusing cytometer Thermo, USA).

10. Primary microglia culture

Brain tissues (neonatal mice within 24 h) were triturated gently and then passed through a 70-μm nylon mesh cell strainer. Cells were re-suspended in DMEM complete medium and seeded into 75 cm flasks at a density of 2×10^5 cells/ml. Primary microglia were isolated from mixed glial cell cultures by shaking (200 rpm for 3–4 h at 37 °C) at 7–10 days after culture.

11. Cell viability assay

The measurements of reduction in 3-(4,5-dimethylthiazol-2-yl)-2,5-diphenyl tetrazolium bromide (MTT; Sigma-Aldrich) were performed to estimate cell viability. MTT was prepared as a 5 mg/ml stock solution in PBS. MTT (5 μl) was added to each well (final concentration 0.5 mg/ml) for 4 h at 37 °C. 24 h after adding different concentrations of EP, the supernatant was then collected for lactate dehydrogenase (LDH) release assay, and then 100 μl DMSO was added to thoroughly dissolve the dark blue crystal formazan. Absorbance was measured after 4 h of culture in a microplate reader at 570 nm by multifunctional Synergy H1 Hybrid Reader (BioTek, USA).

12. Cell death assay

A quantity of 50 μl of each well in the above culture was collected and transferred to a corresponding microtiter plate for LDH release assay. The LDH release was measured using cytotoxicity detection kit (Roche Diagnostics, Mannheim, Germany) following the manufacturer's instructions. Absorbance was detected in a microplate reader at 490 nm by multifunctional Synergy H1 Hybrid Reader (BioTek, USA).

13. Cell migration assay

The cell migration ability was detected using a woundhealing assay. The cells were seeded in a 6-well plate and incubated to 70–80% confluence. A cell-free straight line was then created in the center of the well by scratching with a sterile pipette tip. Cell migration was observed under phase contrast microscope 6 h after EP was added.

14. Myelin purification

Myelin was purified as described by Norton and Poduslo [23]. In brief, adult mice brain was homogenized in 0.32 M sucrose and washed extensively in PBS (pH 7.4) by centrifugation. The pellet was re-suspended in 0.32 M sucrose, layered over 0.85 M sucrose and subjected to centrifugation at 75 000 g for 30 min. Myelin was recovered and suspended in PBS. Protein concentration of the preparation was measured with a BCA-Kit according to the manufacturer's instructions.

15. Myelin debris fluorescent labeling

Myelin debris was re-suspended with a sterile PBS and labeled in 50 μM carboxyfluorescein succinimidyl ester (CFSE) solution for 30 min at room temperature (RT) protected from light. After centrifugation at 14,800g for 10 min at 4 °C. the supernatant was discarded and pellet was washed with PBS for three times. After the final wash, the pellet of myelin debris was re-suspend to 100 mg/ml with sterile PBS. Labeled myelin debris can be store at −80 °C for up to 6 months.

16. Myelin-debris phagocytosis by fluorescence microscopy and fluorescence reader

BV2 microglia (1×10^5/well) were plated in 12-well plates and incubated with CFSE-conjugated myelin debris (5 mg/ml) for 24 h at 37 °C with 5% CO_2. Unphagocytosed myelin-debris was washed out, and level of phagocytosis was observed under fluorescence microscopy and by multifunctional Synergy H1 Hybrid Reader (BioTek, USA) using fluorescence 485 excited light.

17. Flow cytometry

1) The proliferation of cells: Stock solution of CFSE (5 mM diluted in DMSO, Sigma Aldrich) was prepared and the working concentration of 5 μM was diluted in PBS. Cultured BV2 cells ($1x10^6$ cells/ml) were re-suspended with a sterile PBS and labeled in 50 μM CFSE solution for 15 min at 37 °C. After centrifugation, cells were re-suspended in DMEM medium for 24 h at 37 °C with 5% CO_2.
2) The expression of iNOS and Arg1: Cultured BV2 cells ($1x10^6$ cells/ml) were labeled with PE eflour 610 anti-iNOS (BD Bioscience, USA) and PE anti-Arg1 (R&D System, USA) for 30 min at RT. We performed flow cytometry with 10,000 cells per measurement using FACS Canto II flow cytometer (Becton Dickinson Biosciences, San Jose, CA).
3) PI + cells: BV2 microglia (1×10^5/well) were incubated with CFSE-conjugated myelin debris (5 mg/ml) for 24 h at 37 °C with 5% CO^2. Cultured BV2 cells ($1x10^6$ cells/ml) were labeled with PI (Yeasen Biotech, Shanghai, China) for 20 min at RT.

After washing and centrifugation, flow cytometry was used to evaluate proliferation, expression and death of BV2 microglia. Background values obtained with fluorochrome conjugate isotype controls were subtracted. At least 10, 000 events were collected by flow cytometry (Life technologies Attune Nxt acoustic focusing cytometer Thermo, USA).

17.1. Statistical analysis

All statistical analyses were performed by one-way analysis of variance (ANOVA) followed by a Bonferroni post hoc test using GraphPad Prism 5 software (Cabit Information Technology Co., Ltd. Shanghai, China). Results are expressed as the mean ± SEM. P value < 0.05 was considered statistically significant.

18. Results

18.1. EP improved behavioural performance and promoted remyelination

The CPZ model has been extensively used to study demyelination or remyelination in the CNS [24]. It is well known that CPZ feeding leads to selective loss of oligodendrocytes around 2–3 weeks after CPZ feeding, followed by massive demyelination at 4–5 weeks. The design scheme of this study is shown in Fig. 1a. In line with previous reports, the weight of mice was significantly declined in the first week and maintained at a stable but lower weight in subsequent three weeks, as compared to mice with normal diet (Fig. 1b). There was no significant difference in body weight between CPZ and CPZ + EP groups (Fig. 1b).

To confirm the efficacy of EP in CPZ-induced demyelination, mice were i.p. injected with saline or EP (200 μg/200 μl) daily for 2 weeks (Fig. 1a). It has been reported that demyelinating lesions are indicative of anxiety-and depression-like behavior and cognitive impairment [25–27]. Compared with mice with normal diet, behavioral tests

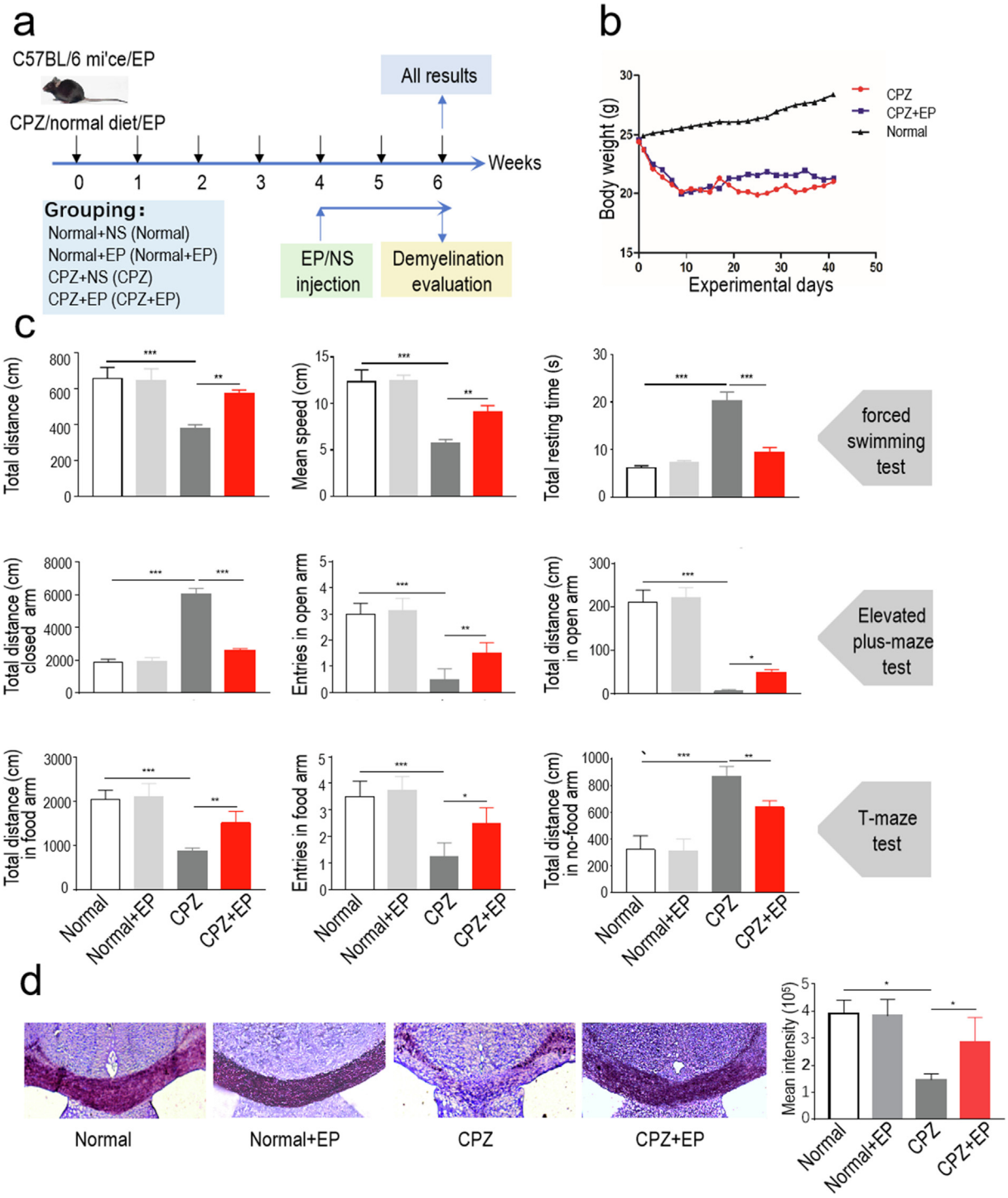

Fig. 1. EP improved behavioral abnormality and reduced demyelination. Mice were fed with chow containing 0.2% CPZ for 6 weeks, and were intraperitoneally injected with EP, starting from fourth weeks until sixth weeks for consecutive 14 days. (a) the design scheme of experimental protocol (n = 8/group), (b) body weight change, (c) anxiety-and depression-like behavior and cognitive function by EPM, FST and T-maze tests, (d) histological evaluation of demyelination by Black Gold II staining. The results were obtained from 3 to 4 mice in each group and quantified by Image-Pro Plus 6.0 software. Micrograph is representative of brain slices in each group with similar results. The results represent the mean ± S.E.M. *$p < 0.05$, **$p < 0.01$, ***$p < 0.001$.

showed that mice fed with CPZ for 6 weeks showed anxiety, depression and cognitive impairment (Fig. 1c). However, EP treatment improved the above behavioral abnormalities as compared with CPZ group (Fig. 1c, $p < 0.05$, $p < 0.01$ and $p < 0.001$, respectively).

Histologically, CPZ-fed mice had a marked demyelinating lesion in the corpus callosum by Black Gold II staining (Fig. 1d, $p < 0.001$). EP treatment increased the intensity of Black Gold II staining compared to CPZ-fed mice (Fig. 1d, $p < 0.001$). These results indicated that CPZ-fed mice showed severe demyelination, which was significantly improved by EP treatment in CPZ-induced demyelinating model.

19. EP influenced microglial phenotype and functions

Microglia are active and dynamic cells that respond quickly to changes in the microenvironment of the CNS. In the acute CPZ model, activated microglia were detected histologically and

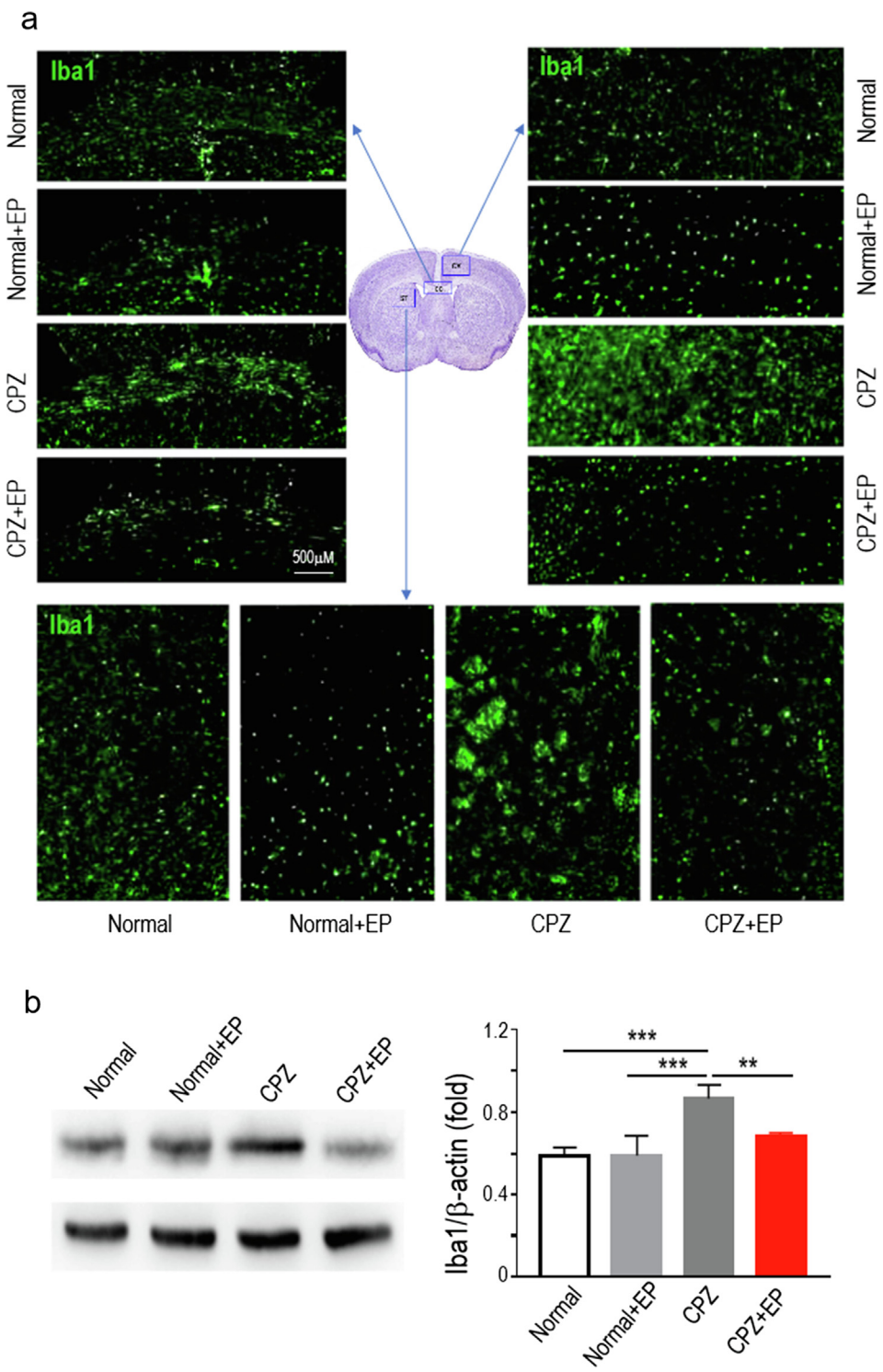

Fig. 2. EP reduced activation and accumulation of microglia in demyelination area. Mice were fed with chow containing 0.2% CPZ for 6 weeks, and were intraperitoneally injected with EP, starting from fourth weeks until sixth weeks for consecutive 14 days. (a) immunohistochemical staining of Iba-1 + microglia in the corpus callosum, striatum and cortex, and b) expression of Iba1 protein in extract of brain by western blot. The results were obtained from 3 to 4 mice in each group and quantified by Image-Pro Plus 6.0 software. Micrograph is representative of brain slices in each group with similar results. The results represent the mean ± S.E.M. $^{**}p < 0.01$, $^{***}p < 0.001$.

immunohistochemically two weeks before demyelination [28]. The results showed that compared with normal mice, CPZ-fed mice represented the enrichment of Iba-1^+ microglia in the corpus callosum, striatum and cortex (Fig. 2a). In brain extract of CPZ-fed mice, the expression of Iba1 was higher than that in normal mice (Fig. 2b, $p < 0.001$). EP treatment obviously reduced the accumulation of Iba-1^+ microglia in the corpus callosum, striatum and cortex and expression of Iba1 in the brain (Fig. 2a and b, $p < 0.01$).

In CPZ-induced demyelination, the cause of microglia enrichment around the myelin sheath is not fully elucidated. Immunohistochemical results showed that Iba1 and MBP double-stained cells existed around the myelin sheath (Fig. 3a). The enlarged image clearly demonstrated that MBP staining was observed in microglia cytoplasm (Fig. 3a, right upper). In addition, the expression of MBP was negatively correlated with the aggregation of Iba1 + microglia (Fig. 3b, right down). These results revealed that the destruction of myelin sheath resulted in enrichment of microglia and phagocytosis of myelin debris.

Because of the fact that the enrichment of microglia in EP-treated mice brain is significantly lower than that in CPZ model mice, we have to carry out in vitro experiments to explore the action of EP regarding the phagocytosis of myelin debris by microglia. First, we screened the reasonable concentration of EP used in vitro experiments by MTT and

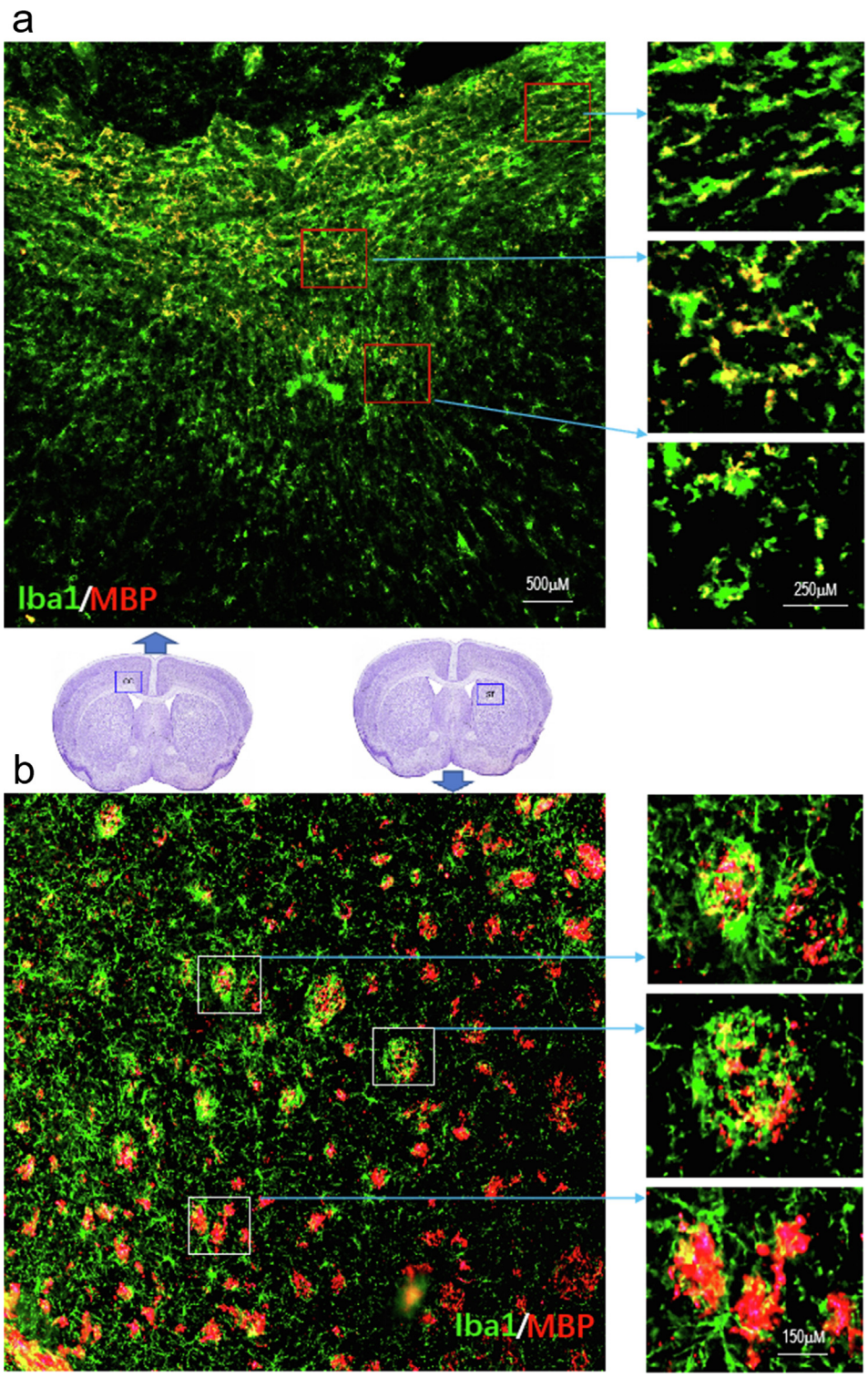

Fig. 3. Microglia engulf myelin debri around the myelin sheaths. Mice were fed with chow containing 0.2% CPZ for 6 weeks, and were intraperitoneally injected with EP, starting from fourth weeks until sixth weeks for consecutive 14 days. Double immunohistochemical staining with anti-Iba-1 and anti-MBP in the corpus callosum a) and striatum b) in CPZ-fed mice. The results were obtained from 3 to 4 mice in each group and micrograph are representative of brain slices in each group with similar results.

LDH methods (Fig. 4a). The concentration (30 μg/ml) was used in the following experiments. EP treatment increased BV2 cell migration (Fig. 4b left), but did not influence BV2 cell proliferation and death by flow cytometry and LDH release (Fig. 4b middle and right). The phagocytic capacity of BV2 cells and primary microglia was analyzed using myelin debris labeled with CFSE after 24 h of treatment. Under fluorescence microscope, BV2 microglia and primary microglia engulfed CFSE-conjugated myelin debris, and the phagocytosis was further increased after EP treatment (Fig. 4c and d). The enlarged image (Fig. 4d) clearly showed that there were many CFSE-labeled particles in the cytoplasm. Compared with control without CFSE-conjugated myelin debris, the fluorescence intensity increased significantly after addition

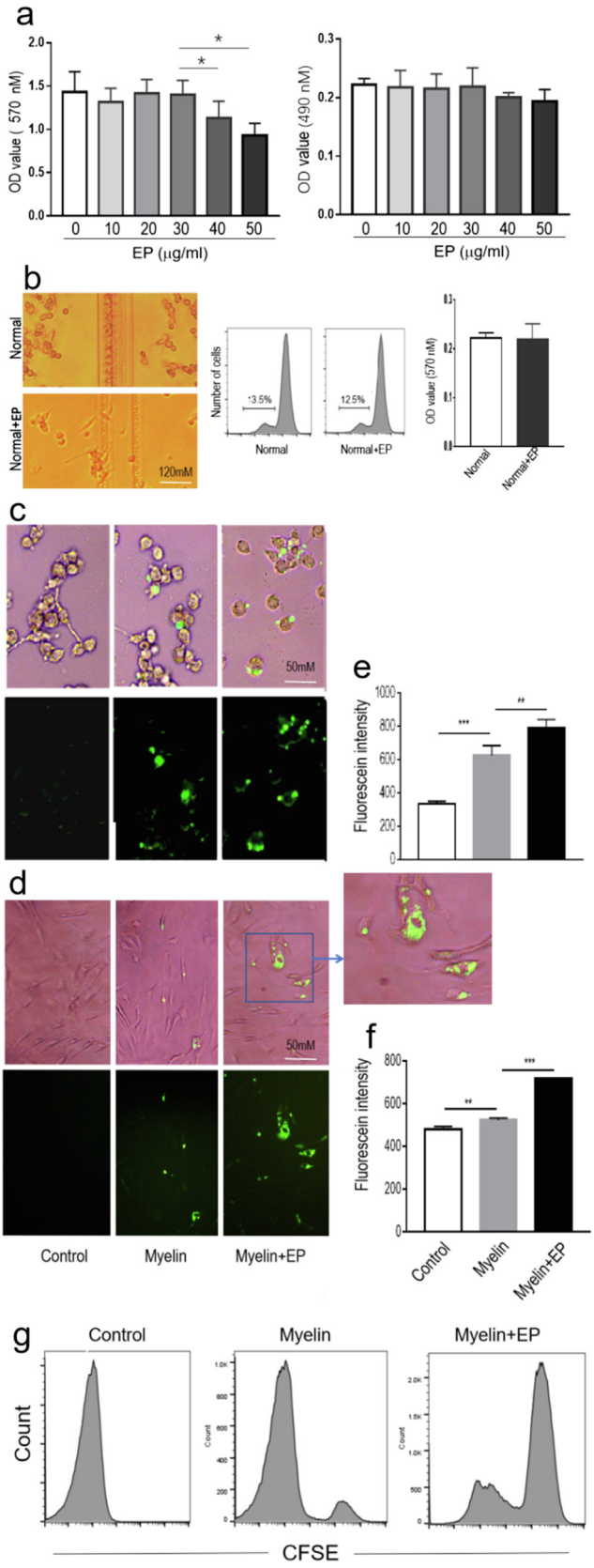

Fig. 4. EP promoted the phagocytosis of myelin debris, (a) the reasonable concentration of EP used in vitro experiments was determined by MTT and LDH methods, (b) the effects of EP on cell migration, proliferation and death were measured by a wound-healing assay, CFSE-proliferation and LDH release, (c and d) the phagocytic capacity of BV2 cells and primary microglia was analyzed using myelin debris labeled with CFSE after 24 h of treatment, (e and f) quantitative analysis of phagocytic CFSE-myelin debris was measured by multifunctional Synergy H1 Hybrid Reader using fluorescence 485 excited light, (g) quantitative analysis of phagocytic CFSE-myelin debris was also measured by flow cytometry. The results were obtained from two independent experiments with similar results. The results represent the mean ± S.E.M. *$p < 0.05$, **$p < 0.01$, ***$p < 0.001$.

of CFSE-conjugated myelin debris (Fig. 4e and f, $p < 0.001$ and $p < 0.01$, respectively). EP treatment further accelerated the phagocytosis of myelin debris by BV-2 microglia and primary microglia (Fig. 4e and f, $p < 0.01$ and $p < 0.001$, respectively). The results from flow cytometry also confirmed that the addition of myelin debris resulted in myelin debris phagocytosis by BV2 microglia (Fig. 4g), while EP promoted markedly BV-2 microglia to engulf myelin debris (Fig. 4g). Taken together, these results clearly indicate that EP can promote the phagocytic capacity of myelin debris by microglia.

Second, after the addition of myelin debris, we observed the morphology, phenotype, proliferation and death of BV2 microglia. The results showed that the expression of iNOS (a M1 microglia marker) decreased, while the expression of Arg1 (a M2 microglia marker) increased after the addition of EP treatment, as compared with control (Fig. 5a). Most interesting, the proliferated BV2 microglia (Fig. 5b, $p < 0.05$) and absolute number of cells (Fig. 5c left, $p < 0.05$) were significantly increased after the addition of myelin debris, and further elevated by EP treatment (Fig. 5b and c left, $p < 0.01$, respectively). LDH release (Fig. 5c right) and flow cytometry (Fig. 5d left) further confirmed that cell death and PI ± cells were elevated after EP treatment ($p < 0.01$ and $p < 0.05$, respectively), as compared with myelin group. However, these PI ± cells were not associated with the phagocytosis of myelin debris (Fig. 5d middle and right). Phase contrast photographs of BV-2 cells in Fig. 5c also showed that EP treatment may increase the death-like BV2 cells (Fig. 3e right, yellow arrow). These results suggest that EP treatment enhanced microglia migration, accumulation and phagocytosis of myelin debris, accompanied by the M2 polarization, proliferation and death of microglia.

20. EP induced M2 microglia and myelin regeneration in vivo

Myelin debris is a pathological substance in the process of demyelination. However, there are still conflicting outcomes of myelin sheath after microglia phagocytosis. Previous studies demonstrated that the speed of remyelination is correlated with the phagocytosis and clearance of myelin debris [29]. Another observation indicated that myelin phagocytosis contributes to damage processes in MS by the associated inflammatory response and oxidative burst [30]. Our results indicated that the expression of inflammatory molecules TLR4 and p-NF-kB/p65 in $Iba1^+$ microglia of mice fed with CPZ was significantly higher than that in normal mice (Fig. 6a and b, $p < 0.01$, respectively), which was inhibited by EP treatment (Fig. 6a and b, $p < 0.01$ and $p < 0.05$, respectively). In accordance with the phenotype of $Iba1^+$ microglia, inflammatory cytokines IL-1β and IL-6 in brain extract of mice fed with CPZ were also significantly higher than those of normal mice (Fig. 6c, $p < 0.001$, respectively). EP treatment effectively reduced the production of inflammatory cytokines in the brain (Fig. 6c, $p < 0.01$, respectively). These results revealed that in the demyelinating region, the microglia that engulfed myelin debris remained mainly inflammatory state.

Although several studies demonstrated that microglia deteriorate the outcome after brain damage in the acute phase, these cells also play a protective role during both the subacute and chronic phases. In vitro experiment, EP treatment induced M2 polarization of microglia by inhibiting iNOS and up-regulating Arg1 (Fig. 5a). In normal mice, EP injection also induced the expression of Arg1 in the corpus callosum

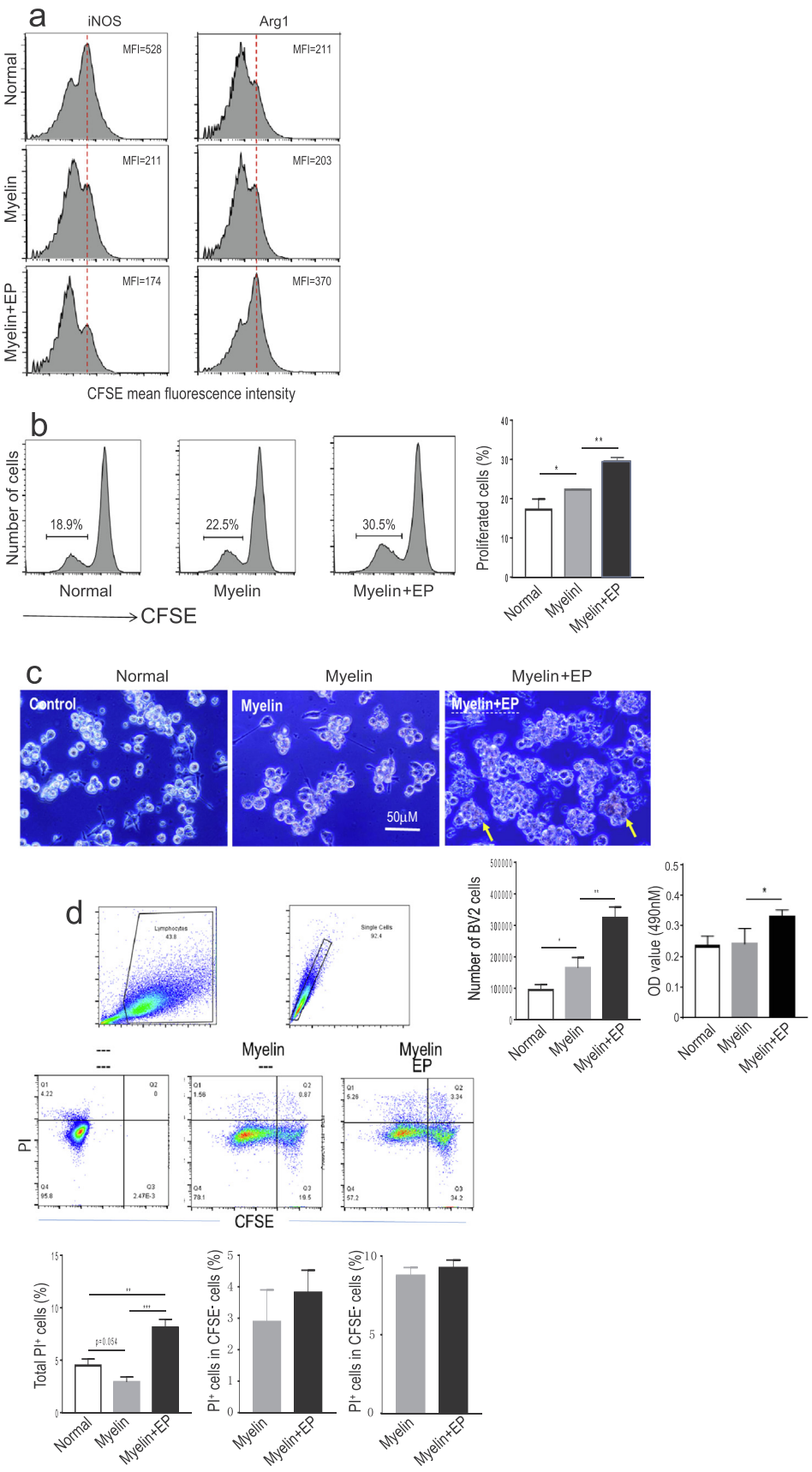

Fig. 5. EP influenced microglial phenotype and functions. Flow cytometry was used to evaluate (a) the expression of iNOS and Arg1 on Iba1 + microglia after addition of myelin debris and EP for 24 h, (b) the proliferation of microglia was measured by CFSE-proliferation assay after addition of myelin debris and EP for 24 h, (c) the morphology of BV2 cells was observed under Phase contrast microscope after addition of myelin debris and EP for 24 h. The absolute number of cells was counted automatically by flow cytometry and the cell death was detected by LDH release assay, (d) percentages of PI + cells in CFSE-/CFSE + cells were measured by double-labeling immunoassay. The results were obtained from two independent experiments with similar results. The results represent the mean ± S.E.M. *$p < 0.05$, **$p < 0.01$, ***$p < 0.001$.

(Fig. 7b, $p < 0.05$), as compared with normal group. In CPZ-model, EP treatment declined the expression of iNOS, and increased the expression of Arg-1 in Iba1$^+$ microglia in the corpus callosum (Fig. 7a and b, $p < 0.05$ and $p < 0.001$, respectively). Next, EP treatment inhibited the production of M1-related TNF-α, and increased the production of M2-related IL-10 in the extract of brain (Fig. 7c, $p < 0.001$,

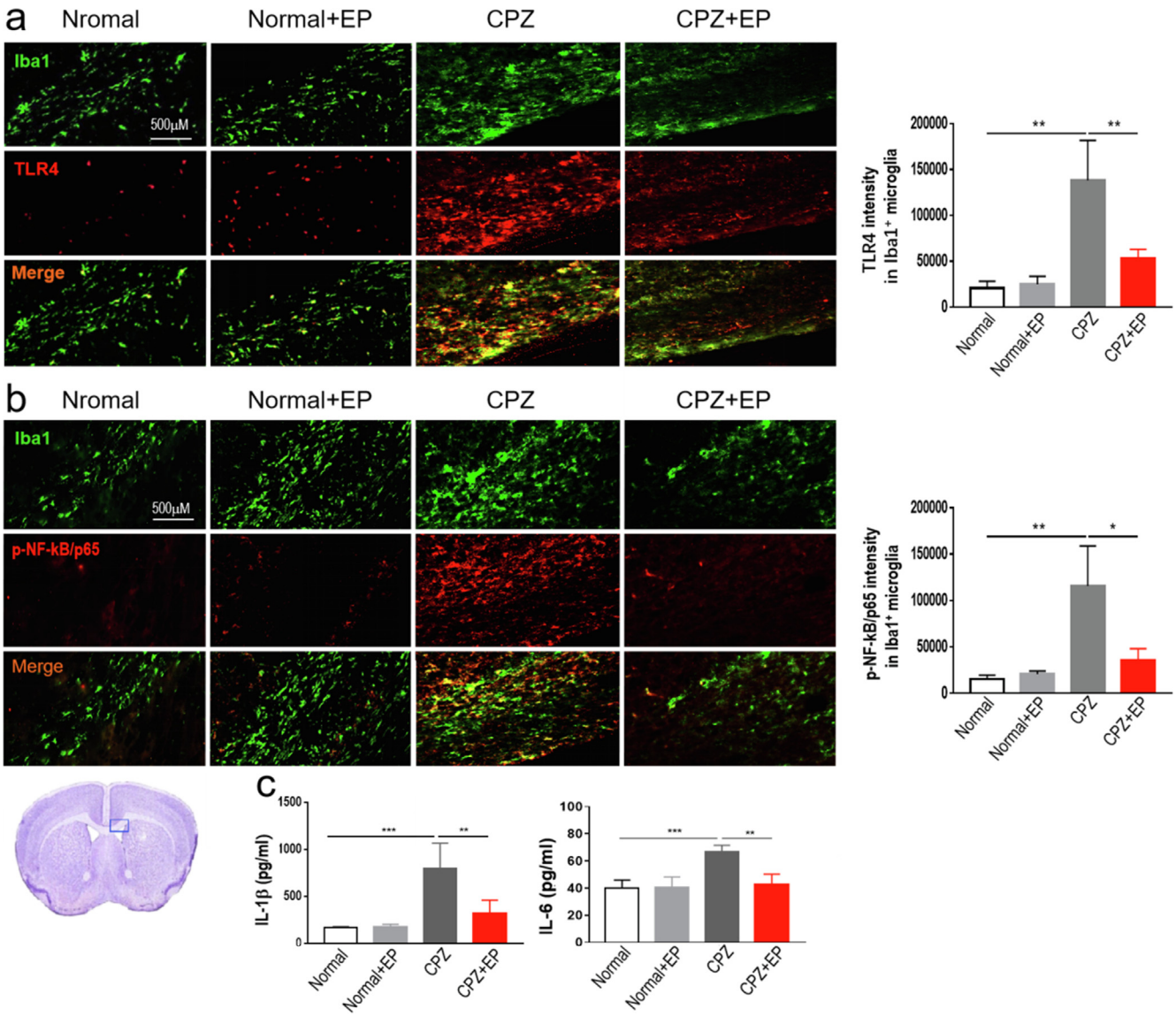

Fig. 6. EP inhibited microglial inflammatory response. Mice were fed with chow containing 0.2% CPZ for 6 weeks, and were intraperitoneally injected with EP, starting from fourth weeks until sixth weeks for consecutive 14 days, (a) double immunohistochemical staining with anti-Iba-1 and anti-TLR4 in the corpus callosum, (b) double immunohistochemical staining with anti-Iba-1 and anti-p-NF-kB/p65 in the corpus callosum, and c) the concentration of IL-1β and IL-6 in extract of brain by ELISA. The results were obtained from 3 to 4 mice in each group and micrograph are representative of brain slices in each group with similar results. The results represent the mean ± S.E.M. *$p < 0.05$, **$p < 0.01$, ***$p < 0.001$.

respectively), revealing that EP treatment induced M2-like polarization in CPZ-induced demyelinating model.

In recent years, many studies have reported that M2 microglia enhance myelin growth and regeneration directly or indirectly. Here, we observed that EP treatment elevated $Olig2^+$ and $NG2^+$ oligodendrocyte progenitor cells (OPCs) (Fig. 8a). The expression of NG2 in the extract of brain was significantly increased after EP treatment (Fig. 8a, $p < 0.05$). Sox2 is essential for oligodendroglial proliferation and differentiation during CNS remyelination [31]. Meanwhile, we also found that EP treatment up-regulated the expression of Sox2 (an essential regulator of oligodendrocyte terminal differentiation) in the lateral ventricles, compared with CPZ-fed mice (Fig. 8b). In addition, EP treatment increased $NG2^+$ OPCs expressing Ki67 (Fig. 8b) in the lateral ventricles, revealing that these $NG2^+$ OPCs are proliferating.

It was observed that NG2 was co-localized on MBP^+ mature oligodendrocytes (Fig. 8c), and enlarged image clearly showed that MBP staining was observed in NG2 OPCs cytoplasm (Fig. 8c, right down). revealing that remyelinating oligodendrocytes express MBP. Simultaneously, the expression of MBP was increased after EP treatment by western blot (Fig. 8e, $p < 0.01$), which was consistent with the result from MBP immunohistochemistry staining (Fig. 8d). These results indicate that EP can promote the regeneration and differentiation of OPCs possibly by inducing the expression of Sox2.

21. Discussion

In this study, we demonstrated that EP improved behavioural performance and promoted myelin regeneration in CPZ-induced demyelinating model. As a possible mechanism of action, EP enhanced microglia migration and phagocytosis of myelin debris, induced cell proliferation and subsequent cell death. In addition, EP induced microglia to exhibit M2 phenotype in vivo and in vitro, accompanied by decreased inflammatory molecules and increased myelin regeneration. As a result, EP treatment induced the generation of OPCs and promoted the differentiation of immature to mature oligodendrocytes, which may be related to the up-regulation of Sox2. To our knowledge, this is the

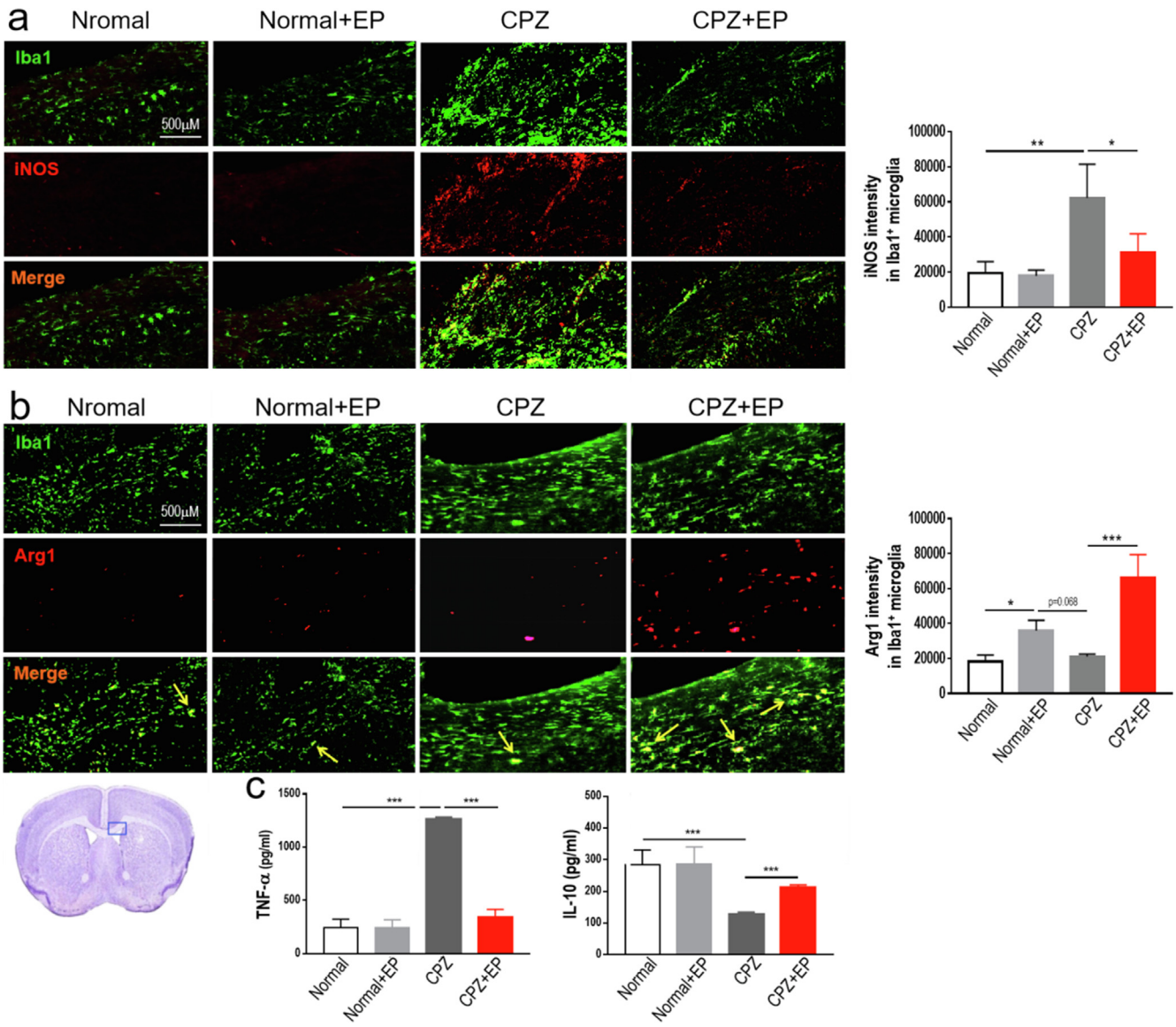

Fig. 7. EP induced polarization of M2 microglia. Mice were fed with chow containing 0.2% CPZ for 6 weeks, and were intraperitoneally injected with EP, starting from fourth weeks until sixth weeks for consecutive 14 days, (a) double immunohistochemical staining with anti-Iba-1 and anti-iNOS in the corpus callosum, (b) double immunohistochemical staining with anti-Iba-1 and anti-p-Arg-1 in the the corpus callosum, and (c) the concentration of M1 TNF- α and M2 IL-10 in extract of brain by ELISA. The results were obtained from 3 to 4 mice in each group and micrograph is representative of brain slices in each group with similar results. The results represent the mean ± S.E.M. *$p < 0.05$, **$p < 0.01$, ***$p < 0.001$.

first study to indicate that EP exhibits therapeutic potential in the treatment and prevention of CNS demyelination.

Microglia maintain homeostasis in the CNS through phagocytic clearance of protein aggregates and cellular debris [32]. Based on the fact that intracranial injection of myelin debris caused the recruitment of microglia [33], we speculate that the destruction of myelin sheath triggers microglia migration and phagocytosis in the corpus callosum, which is further promoted by EP treatment. Microglial phagocytosis can have both beneficial (e.g., debris clearance) and detrimental (e.g., respiratory burst, phagocytosis) consequences [34]. Previous studies suggest that microglia with phagocytic phenotype shifted into an inflammatory response characterized by the secretion of inflammatory IL-1β, IL-6 and TNF-α. Consistent with this result, we also observed that microglia remained in the inflammatory phenotype after the phagocytosis of myelin debris in CPZ model, with increased the expression of TLR4 and NF-kB and the production of IL-1β, IL-6 and TNF- α in the brain. Here, EP treatment enhanced the ability of microglia to phagocytize myelin debris, and accompanied by the decrease of iNOS/TNF- α and increase of Arg-1/IL-10, leading to subsequent myelin regeneration. In EAE, EP treatment resulted in delay and shortening of the first relapse, and lower clinical scores possibly by inhibiting inflammatory cells and cytokines [35]. Recent research showed that rapid clearance of cellular debris by microglia limited secondary neuronal cell death after brain injury in vivo [34]. This discrepancy may reflect differences in the animal models, age, microenvironment, stage of disease and degree of damage in each experiment. However, the cellular and molecular mechanism of EP-induced microglial phagocytosis has not yet been elucidated, which needs to be further explored.

Consistent with our results, an enhanced microglial phagocytosis was accompanied by the polarization of M2 phenotype in the early stage (< 7 days) after intracerebral hemorrhage [36]. Microglia polarization to M2 phenotype is a possible therapeutic target for neurological disorders [37]. This is proposed that M2 microglia/macrophages drive oligodendrocyte differentiation during remyelination and that this is an essential part of an effective remyelination response [38].

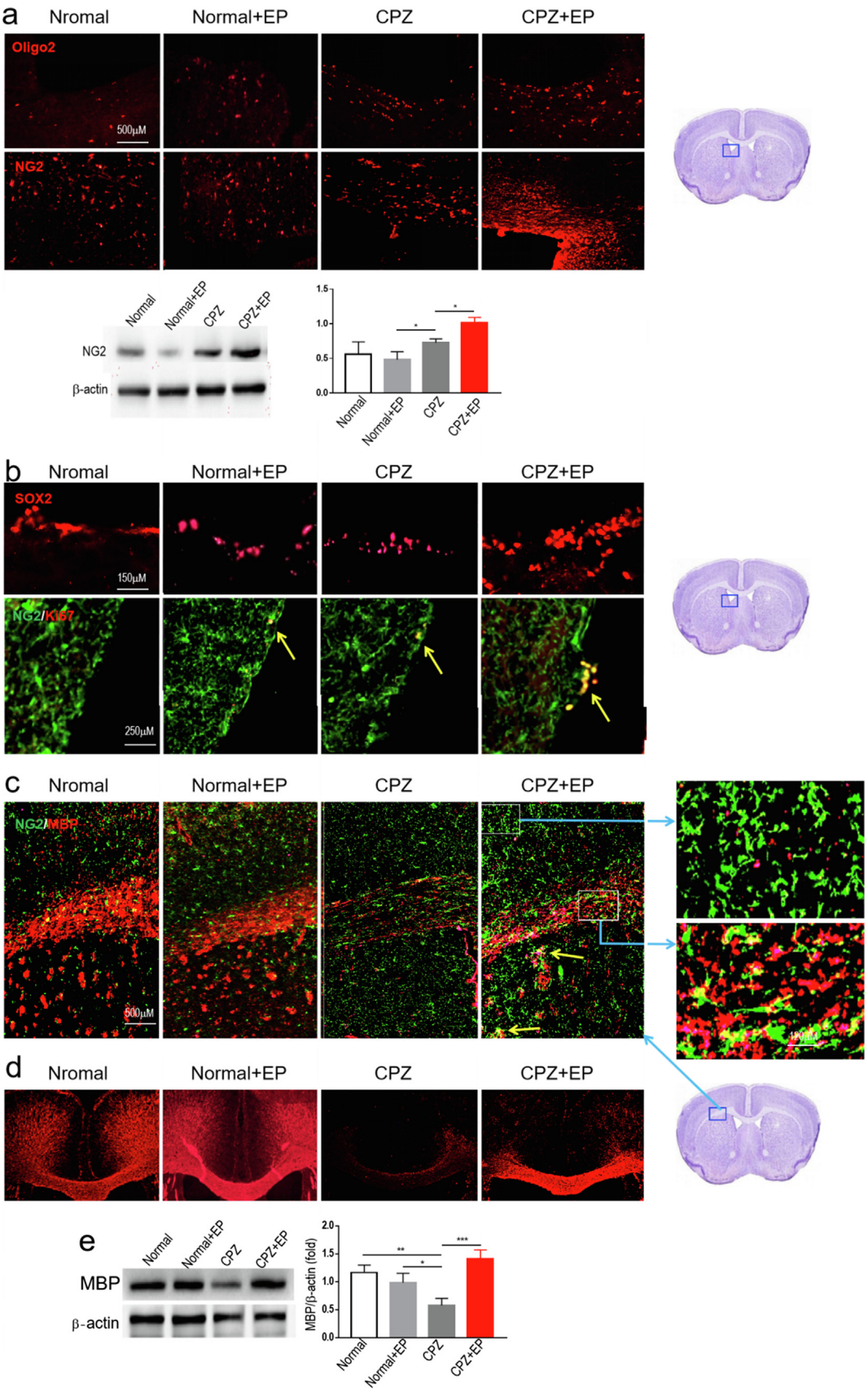

(caption on next page)

Fig. 8. EP induced regeneration and differentiation of oligodendrocyte progenitor cells. Mice were fed with chow containing 0.2% CPZ for 6 weeks, and were intraperitoneally injected with EP, starting from fourth weeks until sixth weeks for consecutive 14 days, (a) immunohistochemical staining with anti-Olig2 and NG2 in the corpus callosum and expression of NG2 in extract of brain by western blot, (b) immunohistochemical staining with anti-Sox2 in the lateral ventricle, and double immunohistochemical staining with anti-NG2 and anti-Ki67 in the lateral ventricle, (c) double immunohistochemical staining with anti-NG2 and anti-MBP around the external capsule, (d) immunohistochemistry staining of anti-MBP, (e) the expression of MBP protein in extract of brain by western blot. The results were obtained from 3 to 4 mice in each group and quantified by Image-Pro Plus 6.0 software. Micrograph is representative of brain slices in each group with similar results. The results represent the mean ± S.E.M. *$p < 0.05$, **$p < 0.01$, ***$p < 0.001$.

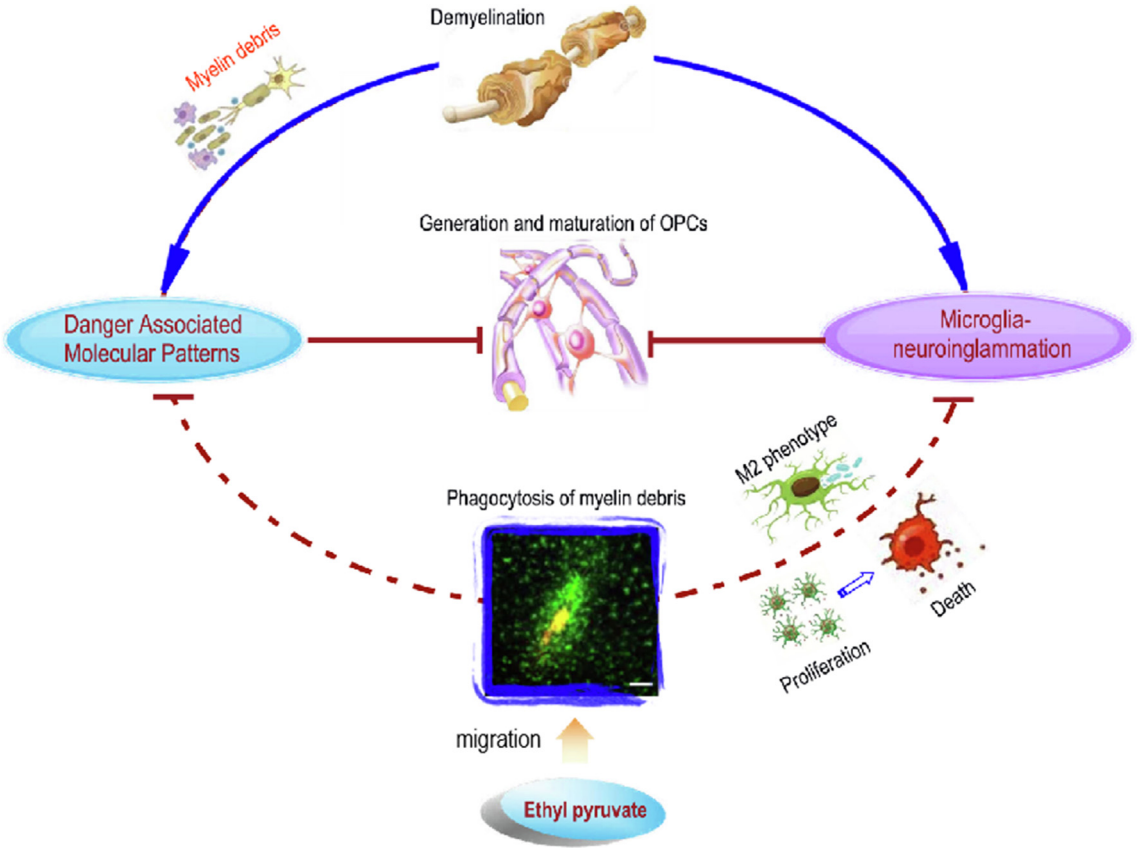

Fig. 9. EP enhanced spontaneous remyelination by targeting microglia phagocytosis. The disruption of myelin sheath results in the production of danger associated molecular patterns (DAMPs), such as myelin debris, and stimulates microglia-mediated neuroinflammation. Both inhibit the generation and maturation of oligodendrocyte precursor cells (OPCs). EP enhanced microglia migration and phagocytosis of myelin sheath debris, induced cell proliferation and subsequent cell death. At the same time, microglia exhibited M2 phenotype, representing anti-inflammatory response. As a result, EP induced the generation of oligodendrocyte progenitor cells and promoted the maturation to mature oligodendrocyte differentiation.

Mechanistically, as remyelination starts, a switch from M1 toward M2 phenotype is observed in microglia populating demyelinated areas. Subsequently, we indeed observed that EP treatment increased $NG2^+$ OPCs and $NG2^+/MBP^+$ mature oligodendrocytes, suggesting that EP not only increased OPCs, but also promoted their differentiation toward maturation. It is now appreciated that phagocytosis is critical in maintaining homeostasis and initiating repair.

During the regeneration and differentiation of myelin sheath, the role of Sox2 in oligodendrocyte biology, and especially in remyelination, is incompletely understood. Sox2 expression occurs in activated OPCs during developmental myelination and remyelination following demyelination. Using both loss-of-function and gain-of-function approaches in cultured OPCs and conditional knockout of Sox2 in transgenic models, Sox2 promoted OPC proliferation and survival [39]. Here, we found that EP treatment induced Sox2 expression, accompanied by increased $NG2^+$ OPCs and $NG2^+/MBP^+$ mature oligodendrocytes in the same region, revealing that Sox2 may be involved in the regeneration and differentiation of myelin sheath. Indeed, we also observed that EP treatment promoted the generation of $NG2^+$OPCs expressing Ki67, revealing that these $NG2^+$ OPCs are proliferating. It is speculated that $NG2^+$ OPCs gradually lose NG2 marker and express MBP during maturation. It is possible that NG2 and MBP may coexist at a particular stage of differentiation. The work by Zhang et al. [31], together with other previous studies, helps to elucidate the function of Sox2 in the complex regulatory network controlling the generation of myelinating oligodendrocytes. Specific deletion of Sox2 in mature oligodendrocytes revealed reduced oligodendrocyte differentiation and myelination in the brain. Surprisingly, this effect was not seen in postnatal spinal cord, suggesting that the regulation of oligodendrocyte differentiation by Sox2 is region-specific [40]. Hoffmann et al. [41] also proposed that Sox2 might function in OPC differentiation. However, it is necessary to verify these findings in vivo and to further define the hypothesis that Sox2 promotes OPC proliferation and differentiation, thereby identifying a possible target for regulating OPC activation and for fostering functional recovery in demyelinating diseases.

Studies from other and our team showed that the density of $Iba1^+$ microglia in the corpus callosum increased significantly after 4 weeks of CPZ feeding. The most striking result in this study, however, was the drastic reduction of $Iba1^+$ microglia in the corpus callosum after EP treatment. It is believed that microglia reactions to injury should be highly dynamic. Our in vitro experiments suggest that microglia can be activated and proliferated after phagocytosis of myelin debris, and then

enter the process of death, which may be the reason for the loss of microglia in the corpus callosum after EP treatment. EP can promote cell migration, but does not affect cell proliferation and death. Therefore, EP-induced cell proliferation and death should be phagocytosis-dependent in direct or indirect manner.

Undoubtedly, there are still many limitations in this study. First, we did not dynamically observe the biological effects of microglia after the phagocytosis of myelin debris; Second, microglial phagocytosis relies on specific receptors expressed on the cell surface and downstream signaling pathways. We will further explore the phagocytic pathways of EP in vivo or in vitro. Third, the relationship between myelin debris phagocytosis, M2 polarization and myelin regeneration also needs to be further studied.

In conclusion, we demonstrated that administration of EP to CPZ-induced demyelinating mice led to an improvement of the behavioural performance and demyelination. In the CPZ model, the possible mechanism of EP is briefly summarized in Fig. 9. Based on these data, we provided the proof-of-experiment that EP may be beneficial in MS or demyelinating lesions. As targeting microglia phagocytosis in neuroinflammatory and demyelinating diseases is receiving increased interest [42], drugs modulating phagocytic capacity may emerge as novel therapeutics for brain disorders. Therefore, further studies on the possibility to use EP as therapeutic application are warranted.

Acknowledgment

This work was supported by grants from the National Natural Science Foundation of China (No. 81371414 and 81473577), and Research Project Supported by Shanxi Scholarship Council of China (2014-7).

Declaration of competing interest

The authors declared that there is no conflict of interest.

References

[1] V. Baecher-Allan, B.J. Kaskow, H.L. Weiner, Multiple sclerosis: mechanisms and immunotherapy, Neuron 2018 (97) (2018) 742–768.
[2] G. Campbell, D.J. Mahad, Mitochondrial dysfunction and axon degeneration in progressive multiple sclerosis, FEBS Lett. 592 (2018) 1113–1121.
[3] R. Martin, M. Sospedra, M. Rosito, B. Engelhardt, Current multiple sclerosis treatments have improved our understanding of MS autoimmune pathogenesis, Eur. J. Immunol. 46 (2016) 2078–2090.
[4] B.D. Trapp, K.A. Nave, Multiple sclerosis: an immune or neurodegenerative disorder? Annu. Rev. Neurosci. 31 (2008) 247–269.
[5] K.A. Nave, Myelination and the trophic support of long axons, Nat. Rev. Neurosci. 11 (2010) 275–283.
[6] A.J. Thompson, S.E. Baranzini, J. Geurts, B. Hemmer, O. Ciccarelli, Multiple sclerosis, Lancet 391 (2018) 1622–1636.
[7] A. Lutterotti, Challenges and needs in experimental therapies for multiple sclerosis, Curr. Opin. Neurol. 31 (2018) 263–267.
[8] K.K. Kao, M.P. Fink, The biochemical basis for the anti-inflammatory and cytoprotective actions of ethyl pyruvate and related compounds, Biochem. Pharmacol. 80 (2010) 151–159.
[9] J.B. Kim, Y.M. Yu, S.W. Kim, J.K. Lee, Anti-inflammatory mechanism is involved in ethyl pyruvate-mediated efficacious neuroprotection in the postischemic brain, Brain Res. 1060 (2005) 188–912.
[10] Y.M. Yu, J.B. Kim, K.W. Lee, S.Y. Kim, P.L. Han, J.K. Lee, Inhibition of the cerebral ischemic injury by ethyl pyruvate with a wide therapeutic window, Stroke 36 (2005) 2238–2243.
[11] Y. Yuan, Z. Su, Y. Pu, X. Liu, J. Chen, F. Zhu, Y. Zhu, H. Zhang, C. He, Ethyl pyruvate promotes spinal cord repair by ameliorating the glial microenvironment, Br. J. Pharmacol. 166 (2012) 749–763.
[12] S.H. Huh, Y.C. Chung, Y. Piao, M.Y. Jin, H.J. Son, N.S. Yoon, J.Y. Hong, Y.K. Pak, Y.S. Kim, J.K. Hong, O. Hwang, B.K. Jin, Ethyl pyruvate rescues nigrostriatal dopaminergic neurons by regulating glial activation in a mouse model of Parkinson's disease, J. Immunol. 187 (2011) 960–969.
[13] Y. Wang, B. Li, Z. Li, S. Huang, J. Wang, R. Sun, Improvement of hypoxia-ischemia-induced white matter injury in immature rat brain by ethyl pyruvate, Neurochem. Res. 38 (2013) 742–752.
[14] J.M. Vega-Riquer, et al., Five decades of cuprizone, an updated model to replicate demyelinating diseases, Curr. Neuropharmacol. 17 (2019) 129–141.
[15] W. Zhen, et al., An alternative cuprizone-induced demyelination and remyelination mouse model, ASN Neuro. 9 (2017) 1759091417725174.
[16] M.E. Witte, L. Bø, R.J. Rodenburg, J.A. Belien, R. Musters, T. Hazes, L.T. Wintjes, J.A. Smeitink, J.J. Geurts, H.E. De Vries, P. van der Valk, J. van Horssen, Enhanced number and activity of mitochondria in multiple sclerosis lesions, J. Pathol. 219 (2009) 193–204.
[17] N. Ohno, H. Chiang, D.J. Mahad, G.J. Kidd, L. Liu, R.M. Ransohoff, Z.H. Sheng, H. Komuro, B.D. Trapp, Mitochondrial immobilization mediated by syntaphilin facilitates survival of demyelinated axons, Proc. Natl. Acad. Sci. USA 111 (2014) 9953–9958.
[18] J.W. Prineas, J.D. Parratt, Oligodendrocytes and the early multiple sclerosis lesion, Ann. Neurol. 72 (2012) 18–31.
[19] J.P. Buschmann, K. Berger, H. Awad, T. Clarner, C. Beyer, M. Kipp, Inflammatory response and chemokine expression in the white matter corpus callosum and gray matter cortex region during cuprizone-induced demyelination, J. Mol. Neurosci. 48 (2012) 66–76.
[20] R.G. Lister, Ethologically-based animal models of anxiety disorders, Pharmacol. Ther. 46 (1990) 321–340.
[21] J.F. Cryan, R.J. Valentino, I. Lucki, Assessing substrates underlying the behavioral effects of antidepressants using the modified rat forced swimming test, Neurosci. Biobehav. Rev. 29 (2005) 547–569.
[22] Y.H. Kim, K.S. Lee, Y.S. Kim, Y.H. Kim, J.H. Kim, Effects of hypoxic preconditioning on memory evaluated using T-maze behavior test, Anim. Cells Syst. 23 (2019) 10–17.
[23] W.T. Norton, S.E. Poduslo, Myelination in rat brain: method of myelin isolation, J. Neurochem. 21 (1973) 749–757.
[24] Q. Liu, W.N. Jin, Y. Liu, K. Shi, H. Sun, F. Zhang, C. Zhang, R.J. Gonzales, K.N. Sheth, A. La Cava, F.D. Shi, Brain ischemia suppresses immunity in the periphery and brain via different neurogenic innervations, Immunity 46 (2017) 474–487.
[25] J. Zimmermann, M. Emrich, M. Krauthausen, S. Saxe, L. Nitsch, M.T. Heneka, I.L. Campbell, M. Müller, IL-17A Promotes granulocyte infiltration, myelin loss, microglia activation, and behavioral deficits during cuprizone-induced demyelination, Mol. Neurobiol. 55 (2018) 946–957.
[26] S. Acharjee, N. Nayani, M. Tsutsui, M.N. Hill, S.S. Ousman, Q.J. Pittman, Altered cognitive-emotional behavior in early experimental autoimmune encephalitis–cytokine and hormonal correlates, Brain Behav. Immun. 33 (2013) 164–172.
[27] Z. Xu, A. Jiang, W. Wang, P. You, D. Lin, X. Li, J. He, Arecoline attenuates memory impairment and demyelination in a cuprizone-induced mouse model of schizophrenia, Neuro Rep. 30 (2019) 134–138.
[28] M.M. Hiremath, Y. Saito, G.W. Knapp, J.P. Ting, K. Suzuki, G.K. Matsushima, Microglial/macrophage accumulation during cuprizone-induced demyelination in C57BL/6 mice, J. Neuroimmunol. 92 (1998) 38–49.
[29] A. Lampron, et al., Inefficient clearance of myelin debris by microglia impairs remyelinating processes, J. Exp. Med. 212 (2015) 481–495.
[30] A. Sierra, O. Abiega, A. Shahraz, H. Neumann, Janus-faced microglia: beneficial and detrimental consequences of microglial phagocytosis, Front. Cell Neurosci. 7 (2013) 6.
[31] S. Zhang, X. Zhu, X. Gui, C. Croteau, L. Song, J. Xu, A. Wang, P. Bannerman, F. Guo, Sox2 Is essential for oligodendroglial proliferation and differentiation during postnatal brain myelination and CNS remyelination, J. Neurosci. 38 (2018) 1802–1820.
[32] J.V. Pluvinage, et al., CD22 blockade restores homeostatic microglial phagocytosis in ageing brains, Nature 568 (2019) 187–192.
[33] T. Clarner, et al., Myelin debris regulates inflammatory responses in an experimental demyelination animal model and multiple sclerosis lesions, Glia 60 (2012) 1468–1480.
[34] C. Herzog, L. Pons Garcia, M. Keatinge, D. Greenald, C. Moritz, F. Peri, L. Herrgen, Rapid clearance of cellular debris by microglia limits secondary neuronal cell death after brain injury in vivo, Development 146 (9) (2019).
[35] D. Miljković, et al., A comparative analysis of multiple sclerosis-relevant anti-inflammatory properties of ethyl pyruvate and dimethyl fumarate, J. Immunol. 194 (2015) 2493–2503.
[36] R. Li, Z. Liu, X. Wu, Z. Yu, S. Zhao, X. Tang, Lithium chloride promoted hematoma resolution after intracerebral hemorrhage through GSK-3β-mediated pathways-dependent microglia phagocytosis and M2-phenotype differentiation, angiogenesis and neurogenesis in a rat model, Brain Res Bull. 152 (2019) 117–127.
[37] C.Y. Xia, S. Zhang, Y. Gao, Z.Z. Wang, N.H. Chen, Selective modulation of microglia polarization to M2 phenotype for stroke treatment, Int. Immunopharmacol. 25 (2015) 377–782.
[38] V.E. Miron, A. Boyd, J.W. Zhao, T.J. Yuen, J.M. Ruckh, J.L. Shadrach, P. van Wijngaarden, A.J. Wagers, A. Williams, R.J.M. Franklin, C. Ffrench-Constant, M2 microglia and macrophages drive oligodendrocyte differentiation during CNS remyelination, Nat. Neurosci. 16 (2013) 1211–1218.
[39] C. Zhao, D. Ma, M. Zawadzka, S.P. Fancy, L. Elis-Williams, G. Bouvier, J.H. Stockley, G.M. de Castro, B. Wang, S. Jacobs, P. Casaccia, R.J. Franklin, Sox2 Sustains Recruitment of Oligodendrocyte Progenitor Cells following CNS Demyelination and primes them for differentiation during remyelination, J. Neurosci. 35 (2015) 11482–11499.
[40] S. Zhang, A. Rasai, Y. Wang, J. Xu, P. Bannerman, D. Erol, D. Tsegaye, A. Wang, A. Soulika, X. Zhan, F. Guo, The stem cell factor Sox2 Is a positive timer of oligodendrocyte development in the postnatal murine spinal cord, Mol. Neurobiol. 55 (2018) 9001–9015.
[41] S.A. Hoffmann, D. Hos, M. Küspert, R.A. Lang, R. Lovell-Badge, M. Wegner, S. Reiprich, Stem cell factor Sox2 and its close relative Sox3 have differentiation functions in oligodendrocytes, Development 2014 (141) (2014) 39–50.
[42] K. Biber, T. Möller, E. Boddeke, M. Prinz, Central nervous system myeloid cells as drug targets: current status and translational challenges, Nat. Rev. Drug Discov. 15 (2016) 110–124.